minerals

MDPI

Article

On the Surface and Beyond. Degradation Morphologies Affecting Plant Ash-Based Archaeological Glass from Kafir Kala (Samarkand, Uzbekistan)

Sara Fiorentino [1,*], **Tania Chinni** [1], **Dagmar Galusková** [2], **Simone Mantellini** [3], **Alberta Silvestri** [4], **Amriddin E. Berdimuradov** [5] **and Mariangela Vandini** [1]

1   Department of Cultural Heritage, University of Bologna—Ravenna Campus, 48121 Ravenna, Italy; tania.chinni2@unibo.it (T.C.); mariangela.vandini@unibo.it (M.V.)
2   Centre for Functional and Surface Functionalized Glass, Alexander Dubček University of Trenčín, 91150 Trenčín, Slovakia; dagmar.galuskova@tnuni.sk
3   Department of History and Cultures, University of Bologna—Ravenna Campus, 48121 Ravenna, Italy; simone.mantellini@unibo.it
4   Department of Geosciences, University of Padova, 35131 Padua, Italy; alberta.silvestri@unipd.it
5   Institute of Archaeology of Samarkand, Uzbek Academy of Sciences, Samarkand 100060, Uzbekistan; uzarchae@mail.ru
*   Correspondence: sara.fiorentino2@unibo.it

Abstract: The study focuses on an assemblage of glass finds from the citadel of Kafir Kala, Uzbekistan, located along one of the major Eurasian branches of the "Silk Roads" with a consistent occupation between the 8th and 12th century CE. Glass fragments for this study were selected based on marked surface alterations they showed, with stratified deposits of different thickness and colours. Starting from a preliminary observation under Optical Microscope, fragments were clustered into four main groups based on the surface appearance of the alterations; Scanning Electron Microscopy investigations of the stratigraphy of the alteration products were then carried out, to evaluate micro-textural, morphological and compositional features. Data from the analyses allowed identifying preferential patterns of development of the various degradation morphologies, linkable to compositional alterations of the glass due to burial environment and the alkali leaching action of the water. Iridescence, opaque weathering (at times associated with black stains), and blackening were identified as recurring degradation morphologies; as all but one sample were made of plant ash-based glass, results show no specific correlation between glass composition and the occurrence of one or the other degradation pattern, often found together. Framed in a broad scenario, the paper aims to set the basis for the development of a study approach dedicated to the degradation morphologies affecting archaeological glasses, a topic still lacking systematisation and in-depth dedicated literature.

Keywords: archaeological glass; Uzbekistan; archaeometry; degradation; SEM-EDS; EPMA

1. Introduction

The present paper focuses on degradation morphologies, identified in glass assemblage from Kafir Kala (Uzbekistan). Glass objects from Kafir Kala are, in fact, affected by severe alteration products, diversified in terms of colours, thickness, and adherence to the surface. In addition to compromising the legibility of the fragments and, thus, hindering their typological study, understanding alterations and the process beyond their occurrence is also interesting from a more strictly scientific perspective. According to current knowledge, it is still unclear to what concomitance of factors the onset and development of different forms of degradation affecting archaeological glass are attributable, nor to what extent they can compromise the durability of glass. To date, much of the investigation into glass deterioration and related mechanisms have been centred around European medieval window glass, while very little attention has been paid to the degradation morphologies

affecting archaeological artefacts [1–15]. Moreover, the use of a tailored vocabulary to describe the visible symptoms of deterioration in the conservation and scientific literature is inconsistent and confusing [10], thus resulting in the lack of a shared vocabulary among scholars and experts from different fields working on archaeological glass studies and conservation.

Ranging from pristine, where no degradation morphology is detectable, to so heavily degraded that most of the original material has transformed into corrosion products, glass finds from archaeological excavations can be unearthed in a variety of conditions. As a material, glass is highly susceptible to the action of water; therefore, when exposed to this agent, the occurrence of degradation phenomena can affect the conservation of glass-made archaeological items. For the same reason, glass objects found in dry soils are generally in better condition than those unearthed from moist soils. Given the presence of water as a necessary condition, the burial environment and the chemical composition of the glass are the two key variables impacting the occurrence and growth of degradation phenomena [2,5,11].

Regarding the burial environment, it has been demonstrated that the chemical degradation of glass is initiated by the attack of water, and it is dependent on its pH value as well [8,12]. Due to the strong polarity of the O-H bonds and the bent shape, the water molecule has a strongly polar character: as the glass interacts with water, the solvent molecules cluster around ions on the glass surface so that positive poles of dipoles seek proximity to anions and negative poles centre over cations. The ions are electrostatically attracted outwards from the glass surface; as a result, the attractive forces between the ions are substantially weakened. More precisely, two key mechanisms, de-alkalinisation (also known as leaching) and network dissolution, contribute to the genesis of alteration layers with compositions different from that of the bulk glass. As explained in detail by Davidson [13], de-alkalinisation occurs since, due to the chemical structure of glass, positively charged alkali and metal cations are free to move around within the glass network. When they are extracted from the glass by water, a sodium or potassium hydroxide solution is formed. To maintain the electrical neutrality of the glass, hydronium ions (H_3O^+) from the water exchange positively charged hydrogen ions for the alkali ions leaching from the glass network. This process results in a hydrated silica-rich surface layer, referred to by several terms: alkali-deficient layer, silica-rich layer, gel layer, or hydrogen glass [3]. Because the hydrogen protons are smaller than the sodium or potassium ions they replace, the alkali-depleted layer will have a smaller volume than the below glass. An electrochemical equilibrium is established first within a few tens of milliseconds. Subsequently, alkali ions (e.g., sodium) are mobilised by excess charge resulting from protons entering the electron cloud of oxygen atoms at the glass surface, forming ≡Si-OH groups immediately. If, for instance, Na^+ is later leached from the glass structure, the remaining matrix cannot contain such high amounts of OH^- groups, and condensation of molecular water in the glass structure occurs [16]. The leached layers can protect the remaining glass from further deterioration, this primarily depends on the composition of the glass and the pH of the leaching solution: in alkaline environments, the silica network is attacked, eventually causing the total dissolution of the glass [14]. Leaching re-occurs cyclically, with additional layers being formed again and overlapping on the glass surface. Moving to network dissolution, this process mainly affects glasses above ground, like windows. If alkali ions accumulate in the leach solution, an increase in the pH value occurs and, when the value of 9 is reached, the breakdown of the network happens. Whereas in the ground alkalis leached from the glass are washed away, in the atmosphere they tend to remain as salts on the glass surface, favouring the breakdown of the network [5].

The rate of deterioration of ancient glasses is influenced by compositional features as well. Glass of a soda-lime-silica composition is almost twice as stable as silica-potash-lime glass: the greater the percentage of alkali, the greater their potential to be extracted [3]. The difference in composition of glass is the reason for the difference in deterioration between relatively stable natron-based glass and less durable plant and wood ash-based ones.

Medieval European glass made from plant and beechwood ash—and, thus, containing higher percentages of potash oxide and alkaline earth to ensure its stability—is highly susceptible to deterioration [13,15]. Soda–lime–silica glassed made by using plant ashes as fluxing agents would seem to be placed in an intermediate position between the more stable, natron-based, and less stable, wood-ash-based ones. The degradation morphologies and related corrosion mechanisms that affect plant ash-based archaeological glass have not, however, been investigated by systematic studies: apart from a study carried out on an assemblage of Sasanian glass finds from Veh Ardašīr, Iraq [7], the chemical processes underlying the degradation of plant ash-based glass are not yet entirely understood. It is, for example, not clear why glass often decomposes in layers and if the layering is linked to cyclic changes, like seasonal variations in temperature and rainfall, and could, therefore, be an indicator of how long the degradation has been in process.

The present study intends to provide insights into morphological, micro-textural, and chemical features of degradation morphologies found on plant ash-based glass finds from Kafir Kala, Uzbekistan. The paper will not deal with the identification and provenance of raw materials used for making the glass, the subject of ongoing research. The manuscript is, instead, aimed at characterising the different types of alterations detected on the analysed finds; framed in a broader context, the study is intended to set the basis for the development of a methodological approach dedicated to the degradation morphologies affecting archaeological glasses, a topic still lacking systematisation, in-depth dedicated literature, and a shared lexicon.

Regarding the site background, the archaeological complex of Kafir Kala is located 12 km southeast of Afrasiab, the ancient city of Samarkand, Uzbekistan (Figure 1a). It is in a strategic position that controlled one of the local north-south passages along the ancient Silk Road (Figure 1b) [17]. The archaeological trenches conducted between the settlement and the Dargom canal (excavation code KK-4) (Figure 1c), and in other parts of the settlement, evidenced sedimentary facies with a noticeable difference in terms of colour and lithology. This difference can be observed between the ochre-red gravel from the local seasonal streams of thick hillslope fan deposits, which form the natural substratum of the settlement, and the dark grey sand originating in the Zeravshan River and borne by artificial canals [18]. The upper citadel (KK-1) was investigated by systematic archaeological excavation by the Uzbek-Italian Archaeological Project—UIAP in different campaigns (2001–2003, 2005–2008, 2013–2014), which provided evidence of two main occupational periods (Figure 1c) [19]. The earliest is dated to the late 7th–early 8th centuries CE, at the time of the conquest of Samarkand by the Arab army; after the conquest, the site was immediately resettled for residential purposes. Alongside the systematic reuse of previous architectural structures, the excavation unearthed the remains of dozens of fire structures (tandir/domed ovens, fireplaces, hearths) and a noticeable quantity of pottery.

Among other classes of artefacts found, coins [20] and glass are the most relevant in number and to understand the Islamic transition this settlement underwent. The glass finds selected for this study belong to three main phases unearthed on the citadel: (1) pre-Islamic, with layers associated with the fire that occurred at the time of the Arab conquest (late 7th–early 8th centuries CE); (2) early Islamic (8th–early 12th century CE); (3) the upper layers indicating post-depositional activities (after 12th century CE)—mainly natural erosion—following the abandonment of the site. An additional sample (KK-d2) comes from 2003 sounding at the western base of the eastern tower at North (excavation code KK3, NEW), which exposed a pottery workshop presumably ascribable to the Timurid period (13th–14th centuries CE).
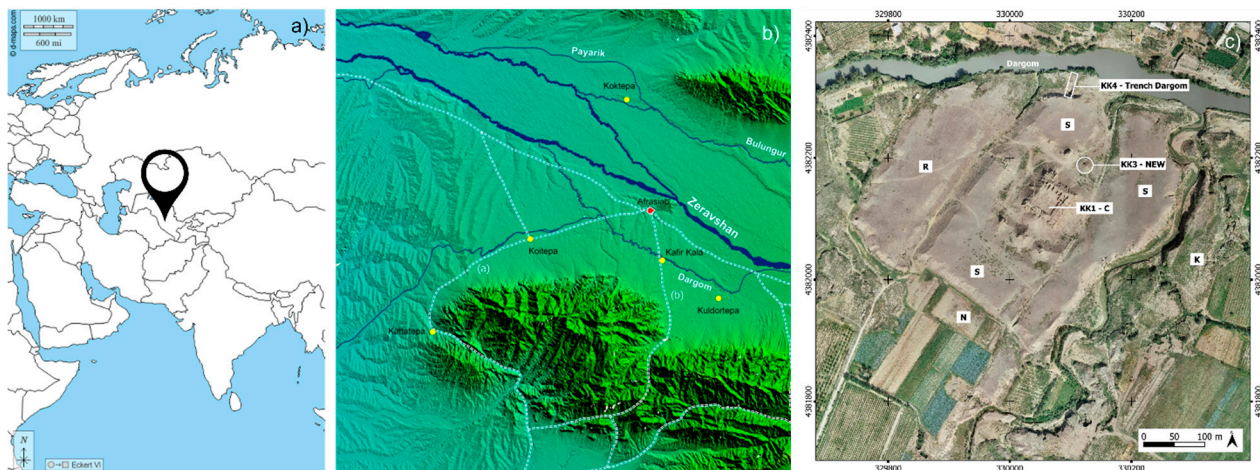
Figure 1. (**a**) location of Uzbekistan (https://d-maps.com/carte.php?num_car=54&lang=it; accessed on 31 October 2021); (**b**) main Silk Road local routes in the Samarkand region (basemap: ASTER GDEM 2013, © UIAP 2015); (**c**) aerial view of the archaeological complex of Kafir Kala with the main excavated areas (drone acquisition and data processing by G. Luglio, © UIAP 2018).

2. Materials and Methods

Among an assemblage of 329 finds, 15 fragments have been selected for in-depth analysis of the degradation phenomena (Table S1). The selection was based on the visual appearance of the degradation patterns: colour, morphology and adhesion to the surface were the main features considered. The following samples were selected for the analyses: KK_d1, KK_d2, KK_d3, KK_d5, KK_h3, affected by iridescence; KK_b2, KK_d4, KK_d6, KK_d7, KK_11, KK_r4, showing opaque weathering; KK_b5, KK_d9, KK_d12, KK_d14 with blackening; black staining was found on samples affected by both iridescence (KK_d5, KK_h3) and opaque weathering (KK_b2, KK_d4, KK_d7, KK_r4).

Glass fragments were analysed by optical microscopy (OM) and scanning electron microscopy coupled with semi-quantitative elemental analysis with an energy dispersion system (SEM-EDS). Preliminary visual inspection and documentation of the finds were performed using a DinoLite USB microscope, with magnification up to $100\times$. An SEM-EDS Quanta Inspect S FEI, equipped with a Philips New XL-30 microprobe, located at the Department of Cultural Heritage, University of Bologna—Ravenna Campus, was used for analysing both the surface of untreated fragments and cross-sectioned samples, to investigate micro-textural and micro-morphological features of the alteration layers. Semi-quantitative elemental analyses were carried out on cross-sectioned samples in high vacuum, on areas and spots for the preliminary characterisation of the base glass and the inclusions; measurements were carried out at 20 kV, with a tungsten filament current of 100 μA, 100 s of acquisition and 10 mm working distance. Due to accessibility problems to the aforementioned SEM-EDS facility, energy dispersion measurements on finds KK_d3, KK-d4, KK_d8 and KK_d12 were performed by using an LEO EVO 40XVP-M Zeiss scanning electron microscope (SEM), connected to an energy dispersion microanalysis system (EDS) INCA Energy 250—Oxford Analytical Instruments Ltd. (UK), available at the Department of Industrial Chemistry, University of Bologna. Analytical parameters were kept the same.

Quantitative chemical analyses, aimed at acquiring data on major and minor elements characterising the pristine glass of Kafir Kala assemblage, were carried out by using electron microprobe (EPMA). To avoid any contamination ascribable to the altered surface, micro-samples (of the order of a few square millimetres) were taken from the core of the selected fragments. To perform EPMA analyses, the glass micro-samples were embedded in blocks of resin. The surface of each block was then polished with a series of diamond pastes down to 1 μm grade and coated with conductive carbon film. The EPMA employed was a JEOL 8200 Super Probe, equipped with five WDS spectrometers and located at the Department

of Earth Sciences of the University of Milan "La Statale". Electron beam operated at 5 nA and 15 KV, with counting times of 30 s for peak and 10 s for background. Standards used for quantitative analyses were grossular for Si, Al and Ca, omphacite for Na, olivine for Mg, K-feldspar for K, rhodonite for Mn, fayalite for Fe, and pure element for Sb. All the certified analyses are available at the Unitech COSPECT of the University of Milan "La Statale".

A preliminary chrono-typological study was also performed on a smaller group of 4 fragments (KK-r4; KK-b2; KK-b5; KK-h3), linkable to specific shapes. Fragment KK-r4 is an everted and flat rim in an emerald green shade, with a diameter of 3 cm. From a chrono-typological perspective, these rims are not particularly informative as they recur in several historical periods and are generally associated with different types of small or large bottles. Rims comparable to fragment KK-r4 can be found among bottles and *unguentaria* from the Roman period [21,22], while subsequent comparisons from Eastern contexts can be identified between the early Islamic material coming from the Ramla train station, the Beirut Souk [23,24] and from the Abbasid strata of Jaffa [25]. Later comparisons can also be found in the Mamluk layers from Quseir al-Qadim (Egypt) [26]. Fragment KK-b2 is a flat bottom with a recessed conoid, in light green glass; the fragment has a mould-blowed honeycomb decoration pattern with a central rosette stamp. Its circumference is about 8.2 cm, a size that is compatible with a bottle or a bowl; this is in line with the literature, identifying the occurrence of this decoration in both open and closed forms, from Abbasid and Fatimid periods in Middle Eastern contexts, testifying the great appeal of the honeycomb decoration [27–30]. Sample KK-b5 is the bottom of a small bottle; the fragment, with a recessed conoid and the pontil mark on the lower surface, has a diameter of 4.8 cm. The original colour of the glass cannot be verified, as the fragment is completely altered. The fragment was unearthed together with a slightly everted rim, indistinct with respect to the wall, having a diameter of about 1.4–1.5 cm; the rim has been attested among assemblages from Jordan and southern Syria, dated to the 7th century AD [31]. Fragment KK-h3 is a ring handle made of blue glass. In ancient glassware, the use of handles is recurrent on cups, lamps or bottles; the closest parallel was found in a long-necked bottle with two ring handles applied along the neck, coming from the late antique layers of the Beirut Souk [24]. However, the model probably remained in use in the following ages, also applied to other types of objects.

3. Results and Discussion

Weathered glass can have a significant variation of appearances, the visual effects most commonly found on the excavated glass being dulling, iridescence, opaque weathering, pitting, cracking, discolouration and blackening [13]. In the perspective of laying the foundations for a more systematic definition of the morphologies of degradation afflicting glass from archaeological excavations and to encourage the use of a well-defined and shared lexicon, the results obtained from the investigations carried out for this study will be presented divided into sub-paragraphs, each dedicated to a specific degradation morphology among those identified on the analysed assemblage.

Except for sample KK-d12, which is completely altered, a preliminary evaluation of quantitative data obtained by EPMA on pristine glass (Table S2) allow characterising all the glass fragments from Kafir Kala as silica-soda-lime, made by using plant ash as fluxing agent (SiO_2 between 58.2 wt% and 67.92 wt%; Na_2O between 14.15 wt% and 18.90 wt%; CaO between 3.66 wt% and 8.96 wt%; K_2O between 2.05 wt% and 6.44 wt%; MgO between 2.74 wt% and 4.98 wt%). The only exception is sample KK_d11 (having K_2O = 0.41 wt% and MgO = 0.48 wt%), made by using natron as a fluxing agent. As this article focuses upon degradation morphologies affecting plant ash-based glass, a more in-depth discussion on compositional data, aimed to establish possible comparisons with assemblages datable to the same chronological frame and unearthed from neighbouring geographical areas, will be carried out in a forthcoming paper.

3.1. Iridescence (without and with Opaque White Weathering)

Iridescence is the first alteration layer found in direct contact with pristine glass. Also named "rainbow iridescence" [14], "rainbow-like effect" [8] or "shelly layer" [32] this morphology of degradation can be distinguished for its peculiar chromatic features: it resembles a thin layer of oil on a water surface, caused by the interference between rays of light reflected from thin alternating layers of air and weathered glass [13].

This degradation morphology has been detected, at different stages, on fragments KK_d1, KK_d2, KK_d3, KK_d5 and KK_h3. Under OM a heterogeneous colouration of the surface can be observed on KK_d1 and KK_d2, with vivid colours in the shades of purple, blue, violet or pink (Figure 2a). Often superimposed, the iridescence layers are extremely thin (a few microns) and highly unstable, with a strong tendency for delamination even during gentle handling. Back Scattered Electrons (BSE) images acquired on the surface of untreated fragments show a laminated structure with a marked cracking network at a micrometric scale. The occurrence of micro-pores with a diameter between 20–35 μm can also be observed (Figure 2b). These crater-shaped structures can be interpreted as preferential sites for capillary infiltration of water and consequent growth of the iridescence layers, resulting, at a later stage, in the so-called "shelly layer" identified by Emami and colleagues [32]. As demonstrated by Silvestri and co-authors [33], the typical iridescence effect of degradation products could be due to ordered periodic nano-lamellar structure which, being characterised by nano-lamellae spacings in the range of the visible-light wavelength, give rise to selective light diffraction processes.
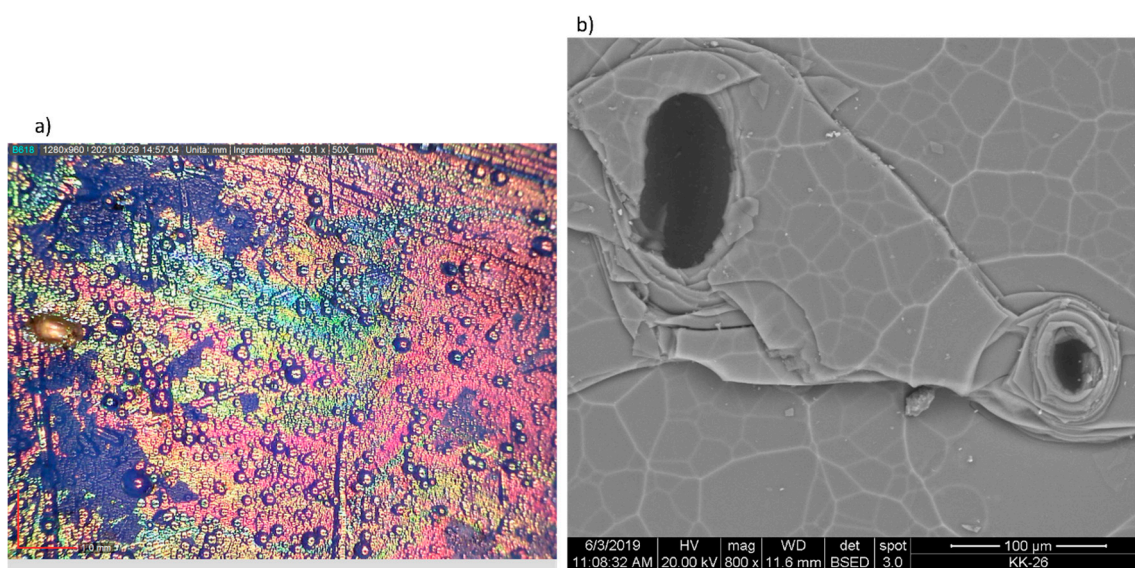
Figure 2. Iridescence on glass fragment KK_d1: (**a**) OM documentation, highlighting the occurrence of bubbles due to the leaching progress followed by pitting; (**b**) BSE image of the surface, with details of the cracking network and a micrometric pore, in the white rectangle.

On samples KK_d3, KK_d5 and KK_h3 iridescence is found at a more advanced state. Under OM, these samples show a much more compact weathering layer compared to KK_d1 and KK_d2, with a pearlescent white appearance and the sporadic occurrence of micrometric black stains, resembling the shape of leaves (Figure 3a,b). Micro-textural and micro-morphological analyses under SEM-BSE allowed gaining further insights into this different type of iridescence: the layer is more compact and devoid of the lamellae conformation observed for KK_d1 and KK_d2 samples (Figure 3c); EDS measurements performed on the black stains showed their hue is ascribable to manganese, whose content ranges between 2.34 wt% and 5.71 wt% (Figure 3d). EPMA data exclude that the manganese found in the black stains had migrated to the surface from the glassy matrix, as samples KK_d3, KK_d5 and KK_h3 all have negligible manganese contents (MnO < 0.04 wt%). The

detected dark stains can be interpreted as the first symptoms of the onset of the morphology of degradation defined as "black staining", which will be discussed in more detail in the dedicated sub-paragraph.
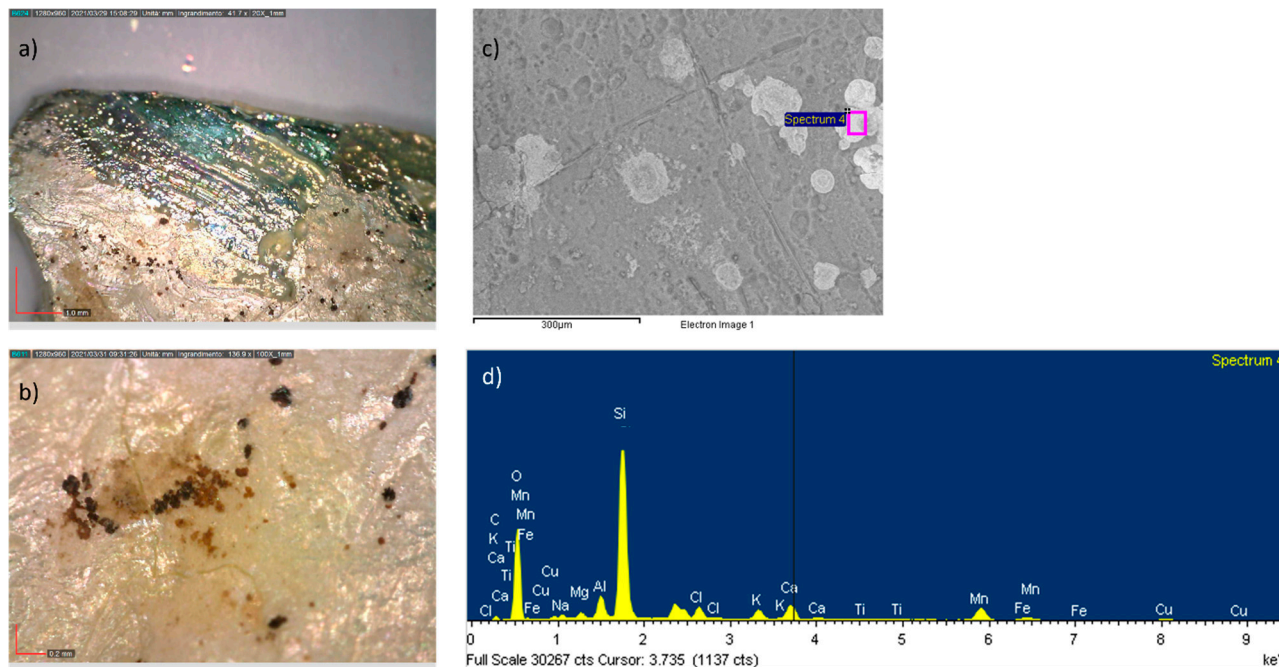

Figure 3. Iridescence on glass fragment KK_d3: (**a**) OM documentation; (**b**) magnified detail of the black stains (100×); (**c**) BSE image of the surface; (**d**) EDS spectrum acquired on the black stains.

3.2. Opaque Weathering

Synonym of "opalescent weathering", the term describes opaque white surface alteration products. The alteration is generally made up of overlapping layers, which develop on the surface of the glass. According to the literature, in its incipient stage, when small whitish spots are only visible on the surface, this degradation morphology is termed "milky" weathering [3]; conversely, at a more severe stage, the alteration is named "enamelline" and it can penetrate inside the glass, eating into it [14]. Opaque weathering also tends to chip off, exposing thinner, iridescent layers below.

In the assemblage of glass finds from Kafir Kala, opaque weathering has been detected on fragments KK_b2, KK_d4, KK_d6, KK_d7, KK_r4. Observation under OM highlighted, on fragment KK_b2, a smooth, opalescent white alteration layer that is not superimposed on the surface but penetrates inside the glass (Figure 4a). BSE images of the stratigraphy confirm a penetration of the alteration layer—having an average thickness of about 570 μm—inside the vitreous matrix, which is being eaten (Figure 4b). Qualitative EDS analysis carried out on the stratigraphic section showed a depletion of Na and decrease of concentration of alkaline earth elements (Ca, Mg), as demonstrated by line scans through the altered surface compared with pristine glass below (Figure 4c).
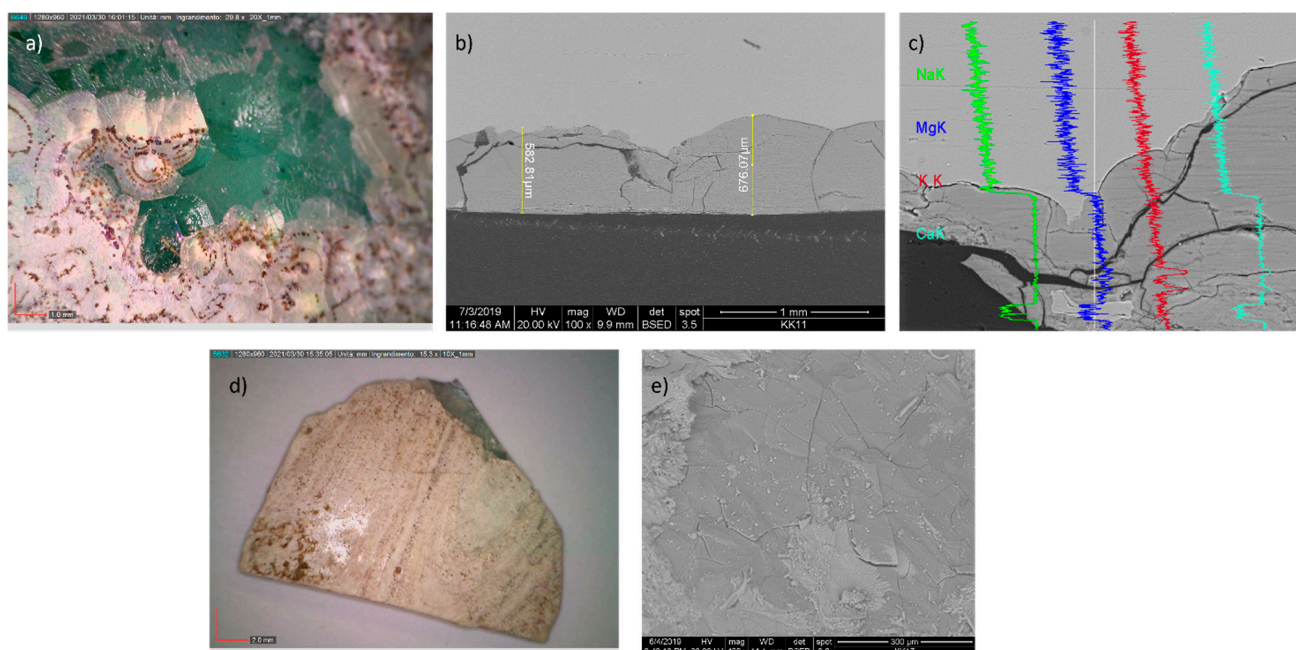
Figure 4. Opaque weathering: (**a**) OM documentation of fragment KK_b2; (**b**) BSE image of KK_b2 cross-section, with detail of the alteration layer penetrating inside the glass; (**c**) EDS line scan through the altered surface and the pristine glass; (**d**) OM documentation of fragment KK_d7, with enamel-like weathering; (**e**) BSE images of fragment KK_d7, untreated sample.

On fragments KK_d4, KK_d6, KK_d7 and KK_r4, opalescent weathering is found at an even more advanced stage. Unlike fragment KK_b2, they are almost entirely covered in a thicker, opaque layer of a whitish colour (Figure 4d). The thickness of the alteration layer is higher, reaching a few millimetres and, as evidenced by the BSE images, it is compact and well adhered to the glass surface (Figure 4e).

All glass fragments from Kafir Kala with opalescent weathering are characterised by small, dark coloured stains on the surface (Figure 4a,d). The occurrence of such dark dots on glass affected by opaque weathering is sometimes reported in the literature, responsible for progressively leading to a colour shift towards brown [3,13,14]. According to data from this study, these spots could be consistent with the so-called "black staining".

Last, a note is deserved by sample KK_d11, showing a degradation pattern that is slightly different, in terms of macro-morphological features, from all the other fragments with opaque weathering. The thin layer of surface alteration is milky and whitish in colour, with a superimposed, spotted iridescence (Figure 5a). EDS mapping and line profile analysis were performed on a cross-sectioned sample (Figure 5b–d). A layer with the evident laminated system as well as semi-circular/oval units originating from the upper surface can be observed: thermal shock followed by physical defects introduced due to technological procedure together with the influence of the environmental burial conditions could be responsible for the deterioration process. Analyses demonstrated that the alteration layer is depleted from sodium and calcium, thus leading to the conclusion that this degradation morphology is ascribable to the leaching of alkaline elements from the glassy matrix.
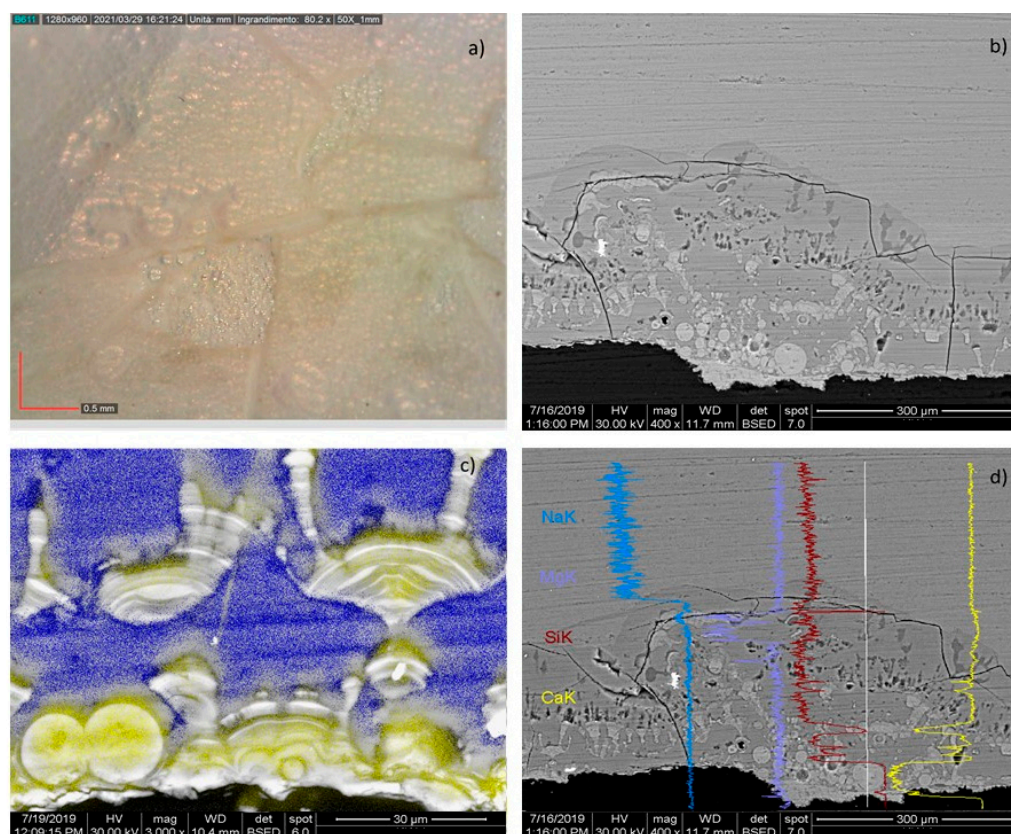
Figure 5. Sample KK_d11: (**a**) OM documentation; (**b**) BSE image of the cross-section, with detail of the alteration layer; (**c**) SEM-EDS mapping, with details of Ca (yellow) and Si (blue) contents; (**d**) EDS line scan through the altered surface and the pristine glass.

3.3. Black Staining and Blackening

Black staining has frequently been observed on both windows and archaeological glass and it is extensively reported in conservation literature [2–5,34–37]. From a morphological perspective, two kinds of staining have mainly been detected: the first feature resembles leaf-shaped deposits on the glass surface, termed dendrites; the second feature is that of micrometric pits, often occurring in concentric ring-shapes.

Dendrites were detected on several fragments from Kafir Kala which, at a first macroscopic examination, had a different appearance: fragments KK_d5 and KK_h3, with severe iridescence; above discussed fragments KK_b2, KK_d4, KK_d7, KK_r4, with opaque weathering; samples KK_b5, KK_d9, KK_d12 and KK_d14, affected by the so-called blackening.

On glass fragments affected by severe iridescence (KK_d5, KK_h3) and opaque weathering (KK_b2, KK_d4, KK_d7, KK_r4), OM images showed that black stains have the actual shape of small leaves, resembling dendrites (Figure 6a–d). SEM-EDS analyses allowed characterising dendrites as mainly made of manganese, the chromophore element responsible for their brown colour and, thus, for the progressive colour shift towards brown and/or black of the alteration noticed on enamel-like alterations by [3,13,14]. As manganese and iron oxides are common soil components, both internal and external sources could be responsible for the black/brown staining of buried archaeological glasses. Watkinson and colleagues [34] carried out laboratory experiments on replicas of potash-based glasses, to simulate the possible effect of dissolved manganese from external environments on scratched, cracked and alkali-leached glass of an archaeological composition without manganese. Results demonstrated that manganese could enter the glass through cracks, forming insoluble brown/black manganese compounds. This corrosion mechanism could explain the occurrence of localised blackening in buried archaeological glass and the dendrite-like inclusions that have been observed. The data obtained from EPMA analyses

of Kafir Kala glass finds support the above hypothesis because fragments with dendritic-shaped growths do not contain intentionally added manganese compounds; MnO contents are negligible, being <0.04 wt% in samples KK_d3, KK_d5, KK_h3, KK_b2, KK_d4, KK_d7 and equal to 0.07 wt% in sample KK_r4.
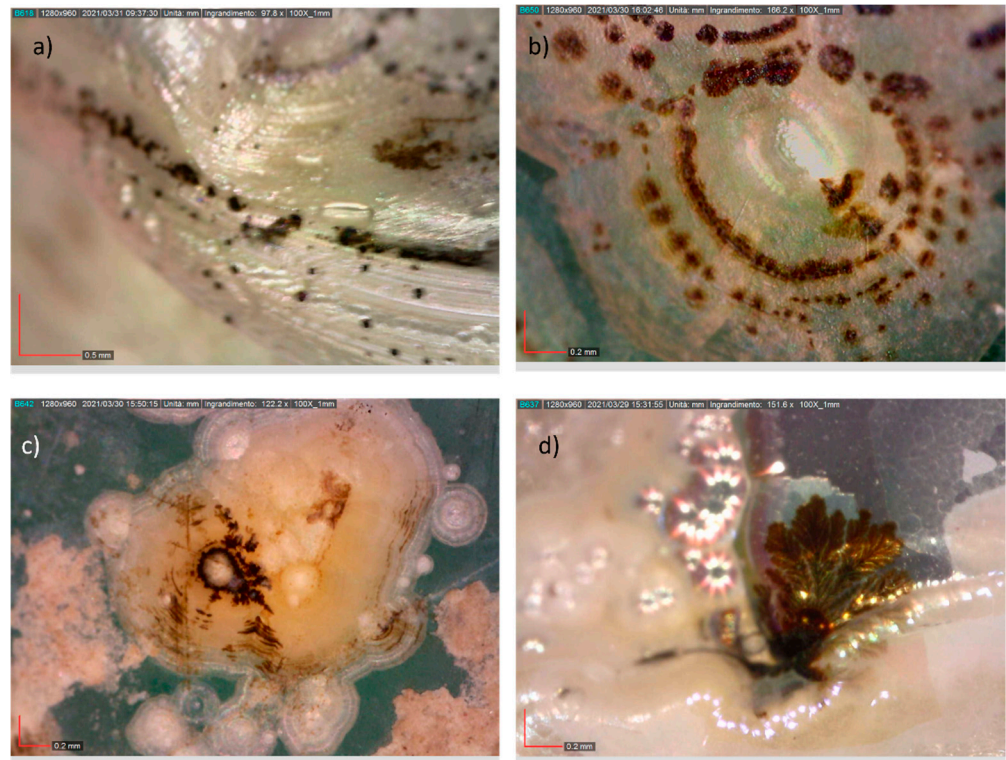
Figure 6. Dark growths in the shape of small leaves detected on fragments, documented under OM (**a**) KK_h3; (**b**) KK_b2; (**c**) KK_d4; (**d**) KK_d7.

Among the assemblage of finds from Kafir Kala, ring-shaped pits were found on green-coloured glass fragments KK_b5, KK_d9, KK_d12 and KK_d14. Upon preliminary visual inspection, the surface of the fragments shows a dark, metallic shade (Figure 7a); images acquired by OM highlight the presence of dark-coloured stains (Figure 7b), which can be found over the entire extension of the surface alteration layer. The observation of the fragments under SEM made it possible to investigate in more detail the micro-morphological and micro-textural features of blackening alteration. BSE images show that the alteration consists of thin, overlapping lamellar layers (Figure 7c); here the occurrence of pits was observed, with circular conformations and having a diameter between 5 and 20 μm (Figure 7d). As demonstrated by EDS spot analysis, the higher electron backscatter shown by these concentric pits is due to an increase in the manganese content, up to 9.30 wt% (Figure 7e).
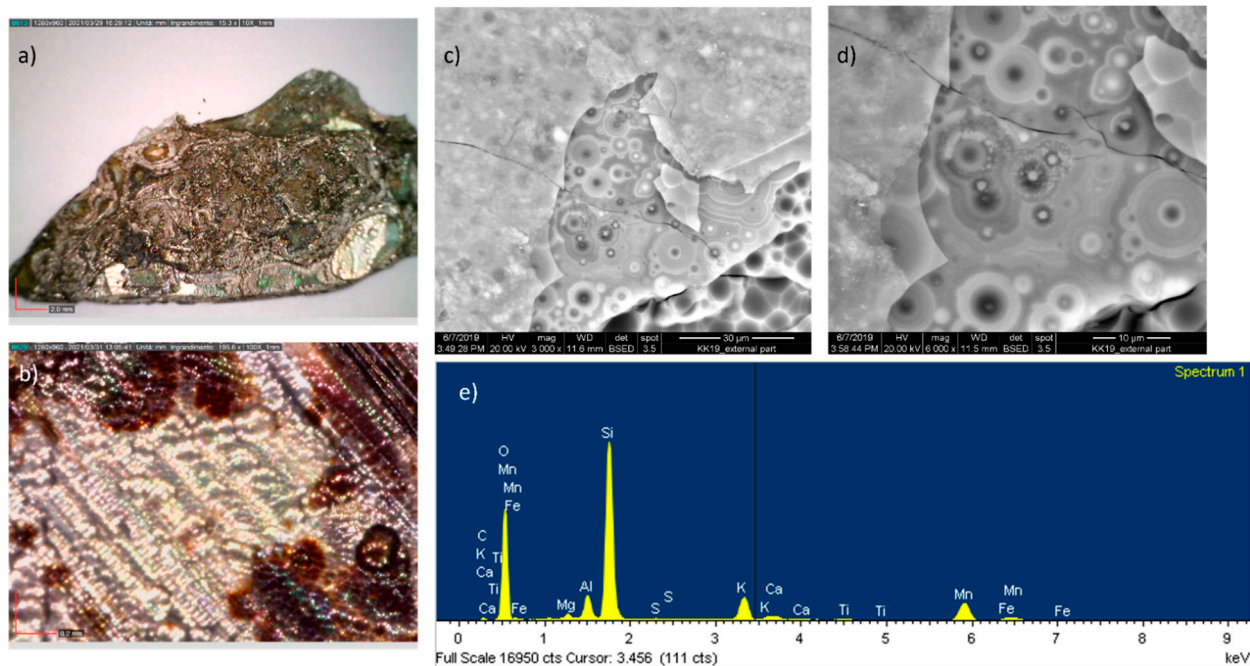
Figure 7. Blackening alteration: (**a**) OM documentation of fragment KK_d12; (**b**) detail of black stains under OM (100×); (**c**,**d**) BSE images of the lamellar structure, with details of concentric pits; (**e**) EDS spectrum acquired on the pits.

SEM-EDS analysis was also performed on micro-samples prepared as stratigraphic sections. BSE images allowed to estimate a thickness of the dark alteration layer, equal to about 500 μm. The layer is made up of several overlapping lamellae, each of a sub-micrometric thickness. The elemental mapping of the chemical composition (Figure 8) highlights a composition mainly made of Si; moreover, it can be observed that the lamellar layers with higher electron backscattering are characterised by Mn enrichment.

As the occurrence of these black stains can also result in an entirely black surface, the term "blackening" has also been found to describe this alteration. According to the literature, three main hypotheses have been formulated regarding the genesis of surface blackening on archaeological glass [1,4]: the oxidation of iron and manganese ions present in the glass; the action of sulphur-reducing bacteria actively producing hydrogen sulphide in anaerobic conditions; the formation of lead sulphide, only occurring in glasses with a high lead content, buried in anaerobic conditions where sulphate-reducing bacteria are producing hydrogen. This darkening effect has mainly been found on medieval potash-based glass, with a tendency to develop dark spots and an opaque lamellar crust during burial, often dark brown or black in colour [3]. Data obtained from EPMA analyses performed on fragments from Kafir Kala are in line with the theory stated by Davidson [3] on the genesis of this blackening effect, ascribable to the oxidation of iron (II) and manganese (II) ions found in the glass; samples KK_b5, KK_d9 and KK_d14 show, in fact, relatively higher manganese contents in the vitreous matrix (MnO ranging between 0.65 wt% and 1.64 wt%) and iron as the only chromoforous ion (FeO ranging between 0.51 wt% and 1.38 wt%). Taking into account that the majority of the analysed samples are pale green in colour, we can hypothesise that the colour is due to iron and manganese dispersed into the vitreous matrix in their reduced state and, because of the leaching process, hydrated Mn (II) and Fe (II) ions are then converted into dark brown MnOOH and FeOOH [38]. Specifically, the concentric circular accretions with a higher manganese content represent preferential sites for the genesis of the leaching of Fe (II) and Mn (II) ions, with consequent formation of a hydrated precipitate held in the pores of the leached hydrated silica layer.
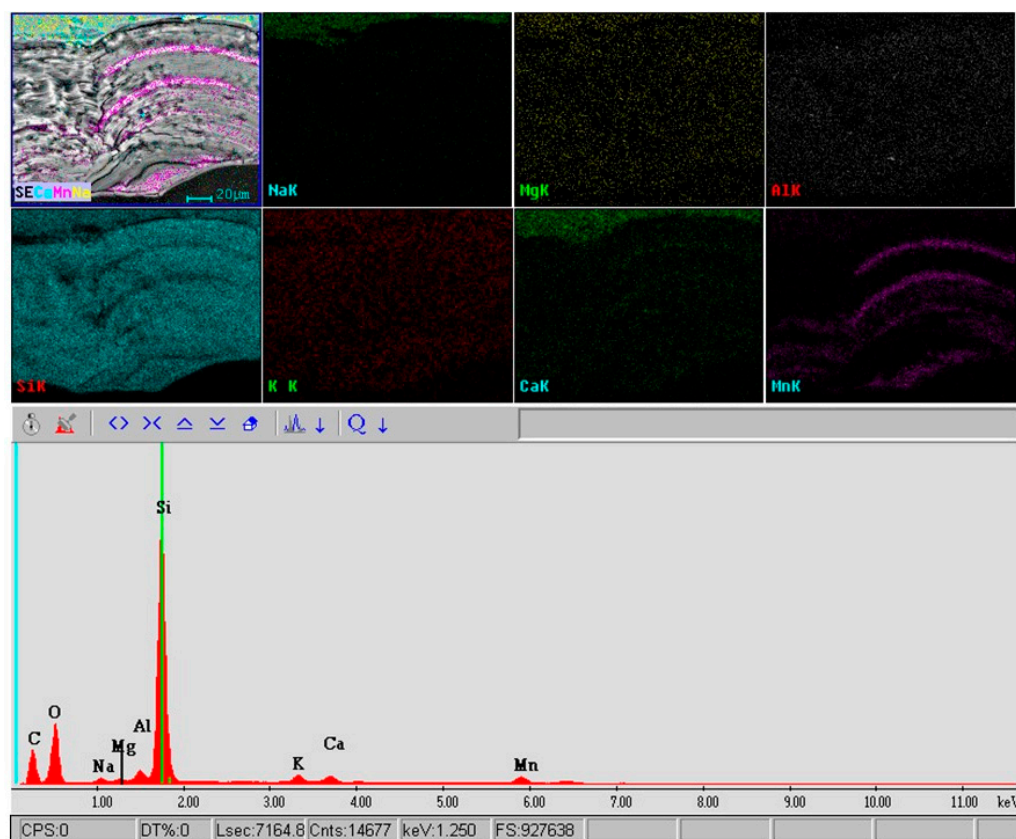
Figure 8. SEM-EDS elemental mapping of the chemical composition (glass fragment KK_d12, cross-section). Scale bar is the same for all subfigures.

4. Conclusions

The study carried out on the degradation morphologies affecting plant ash-based glass set the basis for a preliminary systematisation of the alteration phaenomena found on archaeological glass, moving from a scientific approach to their characterisation and understanding of the underlying dynamics and impacting factors.

The analyses showed that the presence of a single morphology of degradation on the fragments is rarely found as the coexistence of several alteration phenomena is the most frequent occurrence. As for the iridescences, those at a more advanced state (stratified and more adherent to the glass surface) show traces of genesis sites for dendritic growths, the first step towards the subsequent black stains.

All the fragments affected by the so-called opalescent weathering show an alteration with the stratified, lamellar and well-adherent structure to the underlying glass; the latter is also found, in the most severe cases, eaten from the inside. On fragments with opalescent weathering, the presence of preferential sites for the growth of black stains in the shape of dendrites has been observed; here, the conformation of the dendrites begins to be better defined.

Last, concerning the black stains, the following was observed: both the dendritic-shaped and the ring-shaped pits are mainly made up of manganese; however, the processes underlying their formation appear to be different. Regarding the growth of dendrites, the most plausible hypothesis would seem to be the one formulated by [34], stating that manganese could enter the glass through cracks, forming insoluble brown/black manganese compounds. EPMA data support this hypothesis as the presence of MnO in the glass matrix of the samples affected by this degradation morphology was not highlighted. Otherwise, the formation of concentric pits was found exclusively on glass fragments characterised by higher levels of manganese; data support, thus, the theory by Davidson [3] on their genesis, ascribable to the oxidation of iron (II) and manganese (II) ions found in the glass.

References

1.	Shaw, G. Weathered crusts on ancient glass. *New Sci.* **1965**, *27*, 290–291.
2.	Cox, G.A.; Heavens, O.S.; Newton, R.G.; Pollard, M. A study of the weathering behaviour of medieval glass from York Minster. *J. Glass Stud.* **1979**, *21*, 54–75.
3.	Davidson, S. *Conservation and Restoration of Glass*, 2nd ed.; Butterworth-Heinemann: London, UK, 2003.
4.	Knight, B. Excavated Window Glass: A Neglected Resource? In Proceedings of the Archaeological Conservation and Its Consequences, Preprints of the Contributions to the Copenhagen Congress, Copenhagen, Denmark, 26–30 August 1996; Roy, A., Smith, P., Eds.; International Institute for Conservation: London, UK, 1996; pp. 99–104.
5.	Freestone, I.C. Post-Depositional Changes in Archaeological Ceramics and Glasses. In *Handbook of Archaeological Science*; Brothwell, D.R., Pollard, A.M., Eds.; Wiley: Hoboken, NJ, USA, 2001; pp. 615–620.
6.	Silvestri, A.; Molin, G.; Salviulo, G. Archaeological glass alteration products in marine and land-based environments: Morphological, chemical and microtextural characterization. *J. Non. Cryst. Solids* **2005**, *351*, 1338–1349. [CrossRef]
7.	Gulmini, M.; Pace, M.; Ivaldi, G.; Ponzi, M.N.; Mirti, P. Morphological and chemical characterization of weathering products on buried Sasanian glass from central Iraq. *J. Non. Cryst. Solids* **2009**, *355*, 1613–1621. [CrossRef]
8.	Bellendorf, P.; Roemich, H.; Gerlach, S.; Mottner, P.; López, E.; Wittstadt, K. Archaeological Glass: The Surface and Beyond. In Proceedings of the Glass and Ceramics Conservation 2010 Interim Meeting ICOM-CC Working Group, Corning, NY, USA, 3–6 October 2010; ICOM Committee for Conservation: Paris, France, 2010; pp. 137–144.
9.	Majérus, O.; Lehuédé, P.; Biron, I.; Alloteau, F.; Narayanasamy, S.; Caurant, D. Glass alteration in atmospheric conditions: Crossing perspectives from cultural heritage, glass industry, and nuclear waste management. *Npj Mater. Degrad.* **2020**, *4*, 27. [CrossRef]
10.	Gueli, A.M.; Pasquale, S.; Tanasi, D.; Hassam, S.; Lemasson, Q.; Moignard, B.; Pacheco, C.; Pichon, L.; Stella, G.; Politi, G. Weathering and deterioration of archeological glasses from late Roman Sicily. *Int. J. Appl. Glas. Sci.* **2020**, *11*, 215–225. [CrossRef]
11.	Newton, R.G.; Fuchs, D. Chemical analyses and weathering of some medieval glass from York Minster. *Glas. Technol.* **1988**, *29*, 43–48.
12.	Clark, D.E.; Pantano, C.G.; Hench, L.L. *Corrosion of Glass*; Books for Industry: New York, NY, USA, 1979.
13.	Newton, R.G.; Davidson, S. *Conservation of Glass*; Butterworths: London, UK, 1989.
14.	Van Giffen, A. Weathered Archaeological Glass. Available online: https://www.cmog.org/article/weathered-archaeological-glass (accessed on 13 June 2021).
15.	Lombardo, T.; Gentaz, L.; Verney-Carron, A.; Chabas, A.; Loisel, C.; Neff, D.; Leroy, E. Characterisation of complex alteration layers in medieval glasses. *Corros. Sci.* **2013**, *72*, 10–19. [CrossRef]
16.	Bauke, F.G.K. The glass electrode: Applied electrochemistry of glass surfaces. *J. Non. Cryst. Solids* **1985**, *73*, 215–231. [CrossRef]
17.	Mantellini, S.; Berdimuradov, A.E. Archaeological explorations in the sogdian fortress of Kafir Kala (Samarkand region, Republic of Uzbekistan). *Anc. Civiliz. Scythia Sib.* **2005**, *11*, 107–132. [CrossRef]
18.	Malatesta, L.; Castelltort, S.; Mantellini, S.; Picotti, V.; Hajdas, I.; Simpson, G.; Berdimuradov, A.; Tosi, M.; Willett, S. Dating the irrigation system of the Samarkand Oasis: A geoarchaeological study. *Radiocarbon* **2012**, *54*, 91–105. [CrossRef]
19.	Mantellini, S.; di Cugno, S.; Dimartino, R.; Berdimuradov, A.E. Change and Continuity in the Samarkand Oasis: Evidence for the Islamic Conquest from the Citadel of Kafir Kala. *J. Inn. Asian Art Archaeol.* **2016**, *7*, 227–253. [CrossRef]

20. Gariboldi, A.; Mantellini, S.; Berdimuradov, A.E. Numismatic Finds from Kafir Kala as Evidence of the Islamic Transition In Samarkand. In Proceedings of the 5th Simone Assemani Symposium on Islamic Coins, Rome, Italy, 29–30 September 2017; Callegher, B., Rambach, A.D., Eds.; EUT Edizioni Università di Trieste: Trieste, Italy, 2018; pp. 97–126.

21. De Tommaso, G. *Ampullae Vitreae: Contenitori In Vetro di Unguenti e Sostanze Aromatiche Dell'Italia Romana: I sec. a.C.—III sec. d.C.*; Bretschneider Giorgio: Rome, Italy, 1990.

22. Fünfschilling, S. Gläser aus den Grabungen des Deutschen Archäologischen Instituts in Karthago die Grabungen "Quartier Magon" und Rue Ibn Chabâat sowie kleinere Sondagen. In *Die deutschen Ausgrabungen in Karthago*; Rakob, F., Holst, J., Kraus, T., Mackensen, M., Rheidt, K., Stanzl, G.T.O., Vegas, M., Wiblé, F., Wolff, A., Eds.; P. von Zabern: Mainz on Rheine, Germany, 1999; Volume 3, ISBN 3805316798.

23. Ouahnouna, B. RAMLA, Train Station: Glass Finds. In *Hadashot Arkheologigot, Excavations and Surveys in Israel*; Israel Antiquities Authority: Jerusalem, Israel, 2018; pp. 1–16.

24. Jennings, S. Vessel Glass from Beirut BEY 006, 007 and 045. In *Beyruts Archaeological Studies Volumes XLVIII-XLIX 2004–2005, Archaeology of the Beirut Souks 2, AUB and ACRE Excavations in Beirut, 1994–1996*; The Faculty of Arts and Sciences, The American University of Beirut: Beirut, Lebanon, 2006.

25. Ouahnouna, B. Glass Vessels from the Roman, Byzantine and Abbasid Periods at the French Hospital Compound, Yafo (Jaffa). *Atiqot* **2020**, *100*, 211–220.

26. Meyer, C. *Glass from Quseir al-Qadim and the Indian Ocean trade*; Oriental Institute of the University of Chicago: Chicago, IL, USA, 1992.

27. Hadad, S. *Islamic Glass Vessels from the Hebrew University: Excavations at Bet Shean—Excavations at Bet Shean*; Qedem Reports 8; The Hebrew University Of Jerusalem, Institute of Archaeology: Jerusalem, Israel, 2005; Volume 2.

28. Gorin-Rosen, Y. The Islamic Glass Vessels. In *Ramla. Final Report on the Excavations North of the White Mosque*; Gutfeld, O., Ed.; Hebrew University: Jerusalem, Israel, 2010; pp. 213–264.

29. Pollak, R. Excavations in Marcus Street, Ramla: The Glass Vessels. In *Contract Archaeology Reports, II*; University of Haifa: Haifa, Israel, 2007; pp. 100–133.

30. Meyer, C. Sasanian and Islamic Glass from Nippur, Iraq. In Proceedings of the Annales du 13e Congrès de l'Association Internationale pour l'Histoire du Verre (Pays Bas, 1995), Lochem, The Netherlands, 28 August–1 September 1995; Association Internationale Pour L'Histoire du Verre: Amsterdam, The Netherlands, 1996; pp. 247–255.

31. Dussart, O. *Le Verre en Jordanie et en Syrie du Sud*; Institut francais d'archeologie du Proche-Orient: Beirut, Lebanon, 1998.

32. Emami, M.; Nekouei, S.; Ahmadi, H.; Pritzel, C.; Trettin, R. Iridescence in Ancient Glass: A Morphological and Chemical Investigation. *Int. J. Appl. Glas. Sci.* **2016**, *7*, 59–68. [CrossRef]

33. Silvestri, A.; Viti, C.; Molin, G.; Salviulo, G. From Micro- to Nano-Arrangement: Alteration Products in Archaeological Glass from Marine and Land-Based Environments. In Proceedings of the 37th International Symposium on Archaeometry, Siena, Italy, 13–16 May 2008; Memmi Turbanti, I., Ed.; Springer: Berlin/Heidelberg, Germany, 2011; pp. 383–388.

34. Watkinson, D.; Weber, L.; Anheuser, K. Staining of archaeological glass from manganese-rich environments. *Archaeometry* **2005**, *47*, 69–82. [CrossRef]

35. Weber, L.G.; Eggert, G.; Watkinson, D. A closer look at brown staining on archaeological glass. In Proceedings of the Glass and Ceramics Conservation 2007 Interim Meeting ICOM-CC Working Group, Nova Gorica, Slovenia, 27–30 August 2007; ICOM Committee for Conservation: Paris, France, 2007; pp. 35–45.

36. Schalm, O.; Proost, K.; De Vis, K.; Cagno, S.; Janssens, K.; Mees, F.; Jacobs, P.; Caen, J. Manganese staining of archaeological glass: The characterization of mn-rich inclusions in leached layers and a hypothesis of its formation. *Archaeometry* **2011**, *53*, 103–122. [CrossRef]

37. Schalm, O.; Anaf, W. Laminated altered layers in historical glass: Density variations of silica nanoparticle random packings as explanation for the observed lamellae. *J. Non. Cryst. Solids* **2016**, *442*, 1–16. [CrossRef]

38. Möncke, D.; Papageorgiou, M.; Winterstein-beckmann, A.; Zacharias, N. Roman glasses coloured by dissolved transition metal ions: Redox-reactions, optical spectroscopy and ligand field theory. *J. Archaeol. Sci.* **2014**, *46*, 23–36. [CrossRef]